Formation and Destabilization of Actin Filaments with Tetramethylrhodamine-Modified Actin

Dmitry S. Kudryashov, Martin Phillips, and Emil Reisler
Department of Chemistry and Biochemistry, and the Molecular Biology Institute, University of California, Los Angeles, California

ABSTRACT Actin labeling at Cys^{374} with tethramethylrhodamine derivatives (TMR-actin) has been widely used for direct observation of the in vitro filaments growth, branching, and treadmilling, as well as for the in vivo visualization of actin cytoskeleton. The advantage of TMR-actin is that it does not lock actin in filaments (as rhodamine-phalloidin does), possibly allowing for its use in investigating the dynamic assembly behavior of actin polymers. Although it is established that TMR-actin alone is polymerization incompetent, the impact of its copolymerization with unlabeled actin on filament structure and dynamics has not been tested yet. In this study, we show that TMR-actin perturbs the filaments structure when copolymerized with unlabeled actin; the resulting filaments are more fragile and shorter than the control filaments. Due to the increased severing of copolymer filaments, TMR-actin accelerates the polymerization of unlabeled actin in solution also at mole ratios lower than those used in most fluorescence microscopy experiments. The destabilizing and severing effect of TMR-actin is countered by filament stabilizing factors, phalloidin, S1, and tropomyosin. These results point to an analogy between the effects of TMR-actin and severing proteins on F-actin, and imply that TMR-actin may be inappropriate for investigations of actin filaments dynamics.

INTRODUCTION

Actin, which is one of the main components of cellular cytoskeleton, is present in the cell in distinctly different morphological structures, such as individual filaments, filament networks, bundles, stress fibers, and monomers bound to other proteins. Actin cytoskeleton is highly dynamic and can be rearranged rapidly in response to external or internal signals. Frequently, the actin cytoskeleton has been visualized using a high affinity F-actin binding drug phalloidin, labeled with fluorescent markers. However, since phalloidin stabilizes F-actin structure and virtually abolishes the dissociation of actin monomers from filament ends, it also inhibits the dynamic behavior of actin filaments. Moreover, phalloidin competes for the binding to actin with cofilin (Nishida et al., 1987; Yonezawa et al., 1988; McGough et al., 1997)—the actin-binding protein that has a major role in dynamic rearrangements of actin cytoskeleton. Therefore, phalloidin-attached chromophores are not suitable for monitoring the dynamic processes of filament growth, treadmilling, branching, disassembly and severing.

Alternative ways of imaging actin filaments in cells involve the expression of GFP-actin fusion protein (Westphal et al., 1997; Choidas et al., 1998), or the use of actin with fluorescent markers (Hamaguchi and Mabuchi, 1988; Kreis et al., 1982; Bernstein and Bamburg, 1992; Nwe and Shimada, 2000; Yumura and Fukui, 1998). The former approach was used mostly in the in vivo experiments whereas the latter approach was used in both the in vitro and in vivo studies. The small size of the fluorescent probes attached to actin (typically <1 kDa) suggests that they would impair less than GFP (Aizawa et al., 1997; Hosein et al., 2003) the filament structure and/or the binding of other proteins to actin. Among fluorescent dyes, derivatives of rhodamine have been particularly attractive for actin visualization due to their high quantum yield and relative resistance to photobleaching. In most cases, the rhodamine-based probes (tetramethylrhodamine maleimide or tetramethylrhodamine iodoacetomide) were attached to Cys^{374}, the most reactive cysteine on actin. Such a rhodamine-labeled actin was helpful in imaging the in vivo actin dynamics (Sund and Axelrod, 2000; Yumura and Fukui, 1998; Fukui et al., 1999), the in vitro real-time observation of Arp2/3 induced actin filaments nucleation, branching, and growth (Amann and Pollard, 2001; Fujiwara et al., 2002a), and the actin filaments growth and treadmilling (Fujiwara et al., 2002b). Recently, rhodamine actin was used also to reexamine the yield-strength values of single actin filaments (Cintio et al., 2001; Adami et al., 2002), since previous measurements with rhodamine phalloidin-stabilized actin (Tsuda et al., 1996) would have overestimated this value.

Despite the growing use of tetramethylrhodamine maleimide/acetamide modified actins, their polymerization properties have not been described yet. This is particularly important because tetramethylrhodamine maleimide (TMR-maleimide)-labeled actin does not polymerize by itself, without the addition of unlabeled actin (Otterbein et al., 2001; Amann and Pollard, 2001; present study). This property of TMR-maleimide modified actin allowed Otterbein et al. (2001) to solve the first crystal structure of G-actin, free

Submitted March 11, 2004, and accepted for publication May 4, 2004.

Address reprint requests to Dmitry S. Kudryashov, Tel.: 310-825-4585; Fax: 310-206-7286; E-mail: dkudryas@ucla.edu.

Abbreviations used: ANP, *n*-(4-azido-2-nitrophenyl) putrescine; BeF_x, berillium fluoride; DTT, dithiothreitol; EGTA, ethyleneglycol bis(aminoethylether) tetraacetic acid; S1, myosin subfragment 1; SDS-PAGE, sodium dodecylsulphate polyacrylamide gel electrophoresis; TMR, tetramethylrhodamine maleimide/iodoacetamide.

0006-3495/04/08/1136/10 $2.00

doi: 10.1529/biophysj.104.042242

of any actin-binding protein. Also treatment of F-actin with TMR-iodoacetamide, although typically resulting in <50% labeling efficiency (Sund and Axelrod, 2000; Cintio et al., 2001), was shown to disrupt actin filaments (Cintio et al., 2001; Adami et al., 2002), suggesting similar properties for TMR-maleimide- and TMR-iodoacetamide-modified actins. Consequently, it may be expected that copolymerization of TMR-actin with unlabeled actin would produce some perturbation in the actin filament structure. The aim of this study was to evaluate the effect of TMR-actin on the structure and dynamics of copolymers formed from unlabeled and TMR-labeled actin.

In this work, we show that actin filaments containing a high fraction of TMR-actin are significantly shorter, less rigid, and have more bends than the control filaments. The higher fragility of the TMR-actin/unlabeled actin copolymers and the consequent filament severing produce a notably accelerated actin polymerization, most likely due to a higher concentration of free ends available for elongation. This acceleration of polymerization by TMR-actin is abolished by tropomyosin and phalloidin, apparently due to filaments stabilization against severing. Our results suggest that TMR-actin induces significant structural perturbation of the copolymers, even when used at low mole ratios to unlabeled actin.

MATERIALS AND METHODS

Reagents

Tetramethylrhodamine-5-maleimide (TMR-maleimide) and tetramethylrhodamine-5-iodoacetamide (TMR-iodoacetomide) were obtained from Molecular Probes (Junction City, OR). ATP and EGTA and phalloidin were purchased from Sigma Chemical (St. Louis, MO). DTT and HEPES were from Merck (Darmstadt, Germany). PD-10 gel filtration columns were purchased from Amersham Pharmacia Biotech (Uppsala, Sweden). Millipore-filtered water and analytical grade reagents were used in all experiments (Millipore, Billerica, MA). Dolastatin 11, a synthetic F-actin stabilizing drug (Oda et al., 2003), was a generous gift from Dr. R. Bates.

Proteins

Myosin and actin from rabbit back muscle were prepared according to Godfrey and Harrington (1970) and Spudich and Watt (1971), respectively. For light scattering measurements, actin was additionally gel-filtered through a Sephacryl S-200 high resolution matrix (Amersham Pharmacia Biotech) to eliminate traces of oligomers and actin-binding proteins (MacLean-Fletcher and Pollard, 1980). S1 was prepared by digesting myosin filaments with α-chymotrypsin according to the procedure of Weeds and Pope (1977). Protein concentrations were estimated from their absorption by assuming an A (1%) at 280 nm of 7.5 cm^{-1} for S1, and A (1%) at 290 nm in the presence of 0.5 M NaOH of 11.5 cm^{-1} for actin. Whenever appropriate, light scattering corrections were applied. Molecular masses were assumed to be 115 and 42.3 kDa for S1 and actin monomers, respectively.

Cys-374 modification of actin with TMR-maleimide was performed according to the protocol of Otterbein et al. (2001), with minor modifications (Kudryashov and Reisler, 2003). Cys-374 modification of actin with TMR-iodoacetamide was performed similarly, but because of low efficiency of this reaction pure TMR-iodocetamide actin could not be prepared. Briefly, G-actin (5–7 mg/ml) was incubated for 1 h in the presence of 10 mM DTT. Actin was then passed two times through PD-10 (Sephadex G-25) columns to remove DTT, and was incubated overnight with a two molar excess of TMR-iodoacetamide. The labeling was stopped with 2.0 mM DTT and the labeled actin was separated from reagent excess over a PD-10 column pre-equilibrated with G-buffer. The extent of labeling was determined by measuring actin concentration with the Bio-Rad Protein Assay (Bio-Rad laboratories; Hercules, CA), and the concentration of the incorporated TMR using its extinction coefficient at $\lambda = 543$ nm (87,000 M^{-1} cm^{-1}). ANP-crosslinked oligomers were prepared according to Hegyi et al. (1998).

Mg^{2+}-G-actin was prepared by adding 0.4 mM EGTA and 0.1 mM $MgCl_2$ to 5–10 μM Ca^{2+}-G-actin and then incubating the mixture for 10 min on ice. BeF_x-TMR-actin was prepared by incubating ADP-TMR-actin in the presence of 5.0 mM NaF, 0.1 mM $BeCl_2$, and 2.0 mM $MgCl_2$ for 4 h on ice. To prepare Mg^{2+}-TMR-actin/unlabeled actin copolymers for light scattering and calorimetric experiments, both proteins were mixed at the desired mole ratios in the Ca^{2+}-state, then 0.4 mM EGTA and 0.1 mM $MgCl_2$ were added and the samples were incubated for 10 min before the addition of 100 mM KCl and/or 2.0 mM $MgCl_2$.

Light scattering and fluorescence measurements

Light scattering measurements were performed in a PTI spectrofluorometer (Photon Technology Industries, South Brunswick, NJ) with the emission and excitation wavelengths set at 350 nm. Changes in the fluorescence of TMR-actin upon polymerization were detected at $\lambda = 580$ nm after excitation at $\lambda = 544$ nm.

Electrophoresis

SDS-polyacrylamide gel electrophoresis (SDS-PAGE) was performed on 10% gel slabs according to Laemmli (1970). Gels with TMR-actin were visualized under UV light in Alpha-Imager (Alpha Innotech, San Leandro, CA) to reveal the TMR-label, and then stained with Coomassie Blue R-250 to reveal the total protein. The stained gels were scanned using a Scan Premio ST scanner and quantified using the Sigma-Gel software (Jandel Scientific, San Rafael, CA).

Sedimentation experiments

For copolymerization experiments, TMR-actin/unlabeled actin mixtures (20 μM total actin concentration) were incubated for 1.5 h at 23°C in a buffer containing 0.2 mM $CaCl_2$, 0.2 mM ATP, 1.0 mM DTT, and 5.0 mM HEPES (pH 7.5) (G-buffer), and supplemented with 2.0 mM $MgCl_2$. For polymerization with filament stabilizing factors, 5.0 μM TMR-actin was incubated in the G-buffer in the presence of 2.0 mM $MgCl_2$ and one of the following: 10 μM phalloidin, 10 μM dolastatin 11, and 5.0 μM myosin S1. After an incubation for 1.5 h at 23°C, these samples were spun down in the tabletop Beckman airfuge for 30 min at 30 psi. The supernatants and pellets were carefully separated and then denatured for SDS-PAGE analysis. The above experiments were also performed with Mg-G-actin as a starting material, and with 100 mM KCl used in addition to 2.0 mM $MgCl_2$ for the polymerization. None of these factors change by more than 10% the results of the experiments.

Electron microscopy

For EM observation, stabilized Mg-TMR-actin (by S1, phalloidin, etc.) was diluted to 2.5 μM, whereas TMR-actin copolymers, polymerized with 2 mM $MgCl_2$ and in the presence or absence of 100 mM KCl, were diluted to 5.0 μM, and then applied to carbon-coated grids for 60 s, washed by one drop of F-actin buffer and negatively stained with 1% (w/v) uranyl acetate.

A Hitachi H-600 electron microscope was used at an accelerating voltage of 75 kV with a 50-μm objective aperture and a 200-μm condenser aperture at a nominal magnification of 30,000.

Differential scanning calorimetry

Differential scanning calorimetry (DSC) experiments were performed on a 6100 N-DSC II differential scanning calorimeter (Calorimetry Sciences, Provo, UT) with a cell volume of ~0.25 ml. All experiments were performed at a scanning rate of 1°K/min under 3.0 atm of pressure. The total concentration of actin was 60 μM. The reversibility of thermal transitions was checked by a second heating of the sample immediately after cooling, after the first scan. All thermal transitions were irreversible under the conditions used in this study. Because the thermal denaturation of actin was irreversible, only simple thermodynamic parameters and terms were used for the interpretation of the results. The thermal stability of actin was described by the temperature of the maximum of thermal transition (T_m). This parameter can be obtained directly from experimental calorimetric traces after subtraction of the chemical baseline and concentration normalization and, thereby, it can be used for the description of the irreversible thermal denaturation of TMR-actin copolymers.

Analytical ultracentrifugation

1:1, 1:2, and 1:3 mixtures of unlabeled G-actin and TMR-G-actin in the Ca-bound state in G-actin buffer were converted to Mg-G-actin by supplementing the solutions with Mg/EGTA and then polymerizing actin by 2.0 mM $MgCl_2$ for 2 h, at 23°C. Sedimentation velocity experiments were carried out at 20°C in a Beckman Optima XL-A analytical ultracentrifuge equipped with a photoelectric scanning system. Sedimentation boundaries of TMR-actin were recorded at $\lambda = 560$ nm. Boundaries recorded at the beginning of the run, at 3000 rpm, provided the information on total TMR-actin concentration in the solution. Plateau regions of boundaries recorded at the top run speeds (45,000 rpm) contained information on the concentration of TMR-actin that was not incorporated into filaments. At intermediate speeds (30,000 rpm) and run times, the boundaries described all the TMR-actin species present in solution (monomers and polymers). The sedimentation coefficients distribution was determined from a $g(s)$ plot using the Beckman Origin-based software (Version 3.01).

RESULTS

Modification of Cys^{374} on actin with TMR inhibits filament nucleation and elongation

It is recognized that the polymerization of actin in solution consists of three sequential steps: rapid monomer activation; rate-limiting nucleation of new filaments (which appears to be completed with the formation of trimers; Gilbert and Frieden, 1983; Frieden, 1983; Sept and McCammon, 2001); and a relatively fast elongation of the growing filaments (for review, see Estes et al., 1992). The fact that TMR-modified actin was crystallized in the absence of any actin-binding proteins (Otterbein et al., 2001) indicates that at least one step of TMR-actin polymerization is strongly inhibited. Using analytical ultracentrifugation, we found that even after 24-h incubation of 10 μM TMR-actin in the presence of 2.0 mM $MgCl_2$, i.e., under conditions promoting effective polymerization of unmodified actin, >98% of TMR-actin was still in the monomeric state ($s = 3.4 \pm 0.2$S; data not shown). This indicates that TMR-actin does not form oligomers under polymerization conditions. Light scattering experiments confirmed that the addition of 2.0 mM $MgCl_2$ did not cause any significant polymerization of TMR-actin, whereas control actin was readily polymerized under such conditions.

To check whether TMR-labeled actin is capable of elongation, light scattering experiments were carried out in the presence of 1.0 mM $MgCl_2$. At 1.0 mM $MgCl_2$ the elongation rate is only 2.5 times slower, whereas the nucleation is suppressed ~20-fold compared to that at 2.0 mM $MgCl_2$ (Tobacman and Korn, 1983), allowing for better distinction between the elongation and nucleation steps. As expected, neither control nor modified actin (5.0 μM) show any detectable polymerization by 1.0 mM $MgCl_2$ during our observation time (Fig. 1) because of unfavorable nucleation conditions. The addition of 0.2 μM cross-linked actin oligomers—as filament nuclei—causes a prompt increase in the light scattering of control, unlabeled actin, but not for the TMR-modified actin (Fig. 1, *A–B*). This result shows that unlike control actin, TMR-actin alone cannot support a stable elongation process by adding to the preformed filament nuclei.

Copolymerization of TMR-actin and unlabeled actin

Despite the fact that TMR-actin alone does not form filaments or stable oligomers, the addition of unmodified actin leads to the incorporation of TMR-actin into filaments (Fig. 2, Fig. 4 *B*). The fraction of TMR-actin in such

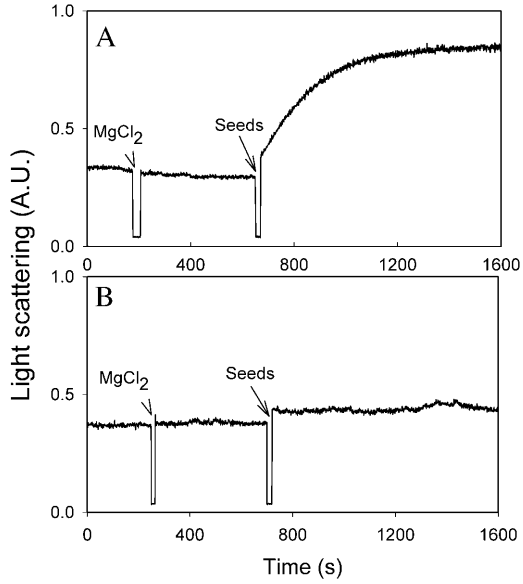

FIGURE 1 Polymerization of unlabeled and TMR-labeled actin by 1.0 mM $MgCl_2$. The time course of polymerization of 5.0 μM unlabeled (*A*) and 5.0 μM TMR-labeled actin (*B*) was monitored by light scattering at 350 nm. Additions of 1.0 mM $MgCl_2$ and 0.2 μM ANP-crosslinked oligomers (seeds) are indicated by arrowheads and arrows, respectively.

copolymers can be estimated from measurements of actin distribution (after ultracentrifugation) between the supernatant and pellet fractions on SDS-PAGE. Only TMR-actin, and not unlabeled actin, is visualized on unstained gels under UV light. On the other hand, Coomassie blue staining allows for monitoring both the labeled and unlabeled actin. Using this procedure, we determined the percentage of TMR-actin content in the copolymers with unlabeled actin in the presence of 2.0 mM $MgCl_2$ at different ratios of labeled/unlabeled actin (Fig. 2 *A*).

However, the above pelleting method may underestimate the fraction of TMR-actin in the copolymers, especially if short filaments and oligomers, which are not easily pelleted, are formed upon copolymerization. To test for the presence of such oligomers, we analyzed the copolymerized mixtures of TMR-actin/unlabeled actin (at 1:1; 2:1; and 3:1 mole ratios) by analytical ultracentrifugation. The results of this experiment clearly show that only monomers and filaments (with sedimentation coefficients of 3.4S and between 30S and 90S, correspondingly), but not oligomers, are present in the copolymerized mixtures of TMR-actin and unlabeled actin (Fig. 2, *B–C*). Furthermore, the fractions of TMR-actin incorporated into copolymers, as calculated from the sedimentation velocity boundaries recorded in these experiments (see Materials and Methods for details), are in good agreement with the data derived from pelleting experiments (Fig. 2 *A*). The sedimentation velocity experiments revealed also that the increasing mole ratios of TMR-actin/unlabeled actin result in the shortening of filaments. This was indicated by the shift in the sedimentation coefficient distributions to lower values (from ~60s to ~35s for the main fraction in the 1:1 and 3:1 mole ratios of TMR-actin/unlabeled actin copolymers, respectively; Fig. 2, *B–C*).

According to these results, the fraction of TMR-actin in the copolymers did not exceed ~50% of the sedimented actin (F-actin), even at high molar excess of TMR-actin over unlabeled actin (9:1). Therefore, it would appear that on average filaments can accommodate TMR-actin at most at an alternating basis with unlabeled actin.

Emission spectra of TMR-actin—before and after its copolymerization with unlabeled actin—show ~50% fluorescence increase upon actin polymerization. This fluorescence increase is linear with the increase in the fraction of TMR-actin incorporated in the copolymers and may be used along with light scattering for monitoring the polymerization reaction (data not shown).

Myosin S1, phalloidin, and BeF_x promote the polymerization of TMR-actin

To clarify whether TMR-actin can be induced to polymerize in the absence of unlabeled actin, we investigated the polymerization of TMR-actin in the presence of myosin subfragment 1 (S1), phalloidin, dolastatin 11, and BeF_x, all of which are known to stabilize the filament structure. As expected, no detectable amount of TMR-actin was found in the pellet, after actin incubation in the presence of 2.0 mM $MgCl_2$ and high speed centrifugation (Fig. 3, Mg^{2+}). Dolastatin 11, which has recently been shown to bind between the two long-pitch strands of actin filaments and thereby stabilize them (Oda et al., 2003; Bai et al., 2001), results in the pelleting of only a small percentage of total TMR-actin (Fig. 3).

Addition of phalloidin or BeF_x leads to a partial stabilization of TMR-actin filaments (Fig. 3, $MgCl_2$ + Phalloidin; $MgCl_2$ + BeF_x). The fraction of TMR-actin pelleted in the presence of phalloidin typically did not exceed 50% under our experimental conditions, and the BeF_x-induced polymerization was even less pronounced. In contrast, equimolar amounts of S1 caused the polymerization of >90% of total TMR-actin, irrespective of the $MgCl_2$ presence (Fig. 3, Mg^{2+} + S1; no Mg^{2+} + S1). The resulting polymers have the general appearance of S1-decorated F-actin (Fig. 4 *C*), although these filaments may be less rigid and less straight than control filaments. Light scattering measurements showed that the S1-induced polymerization of TMR-actin has a characteristic, initial lag phase with no apparent changes in light scattering (data not shown), similar to previous observations with unlabeled G-actin and S1 (Miller et al., 1988). The duration of this phase increased with ATP concentration, which prevents strong binding of S1 to G-actin; the hydrolysis of ATP by S1 present in the solution resulted in the fast polymerization of TMR-actin. Additions of fresh ATP to TMR-actin polymerized by S1 caused almost immediate decrease in the light scattering to that of the monomer actin, indicating fast disassembly of S1-decorated TMR-actin filaments. In unmodified F-actin, which has been assembled by S1, the dissociation of S1 by ATP does not cause a similar rapid depolymerization of filaments (data not shown).

Electron microscopy of TMR-actin/unlabeled actin copolymers

Electron microscopy examination of TMR-actin/actin copolymers was carried out on samples with a known fraction of TMR-actin in the filaments (as determined by the sedimentation and SDS PAGE analysis). Filaments containing ~30% TMR-labeled protein (Fig. 4, *B*, *E*, and *F*) are much shorter than the control filaments (Fig. 4 *A*). Observation of several fields revealed that most of the filaments of unlabeled actin were several micrometers long, whereas most of the TMR-actin copolymers were shorter than 0.5 μm, and <10% exceeded the length of 1.0 μm. Moreover, the structure of the copolymers is perturbed strongly, revealing a tendency of these filaments to form multiple sharp bends (Fig. 4 *E*). Addition of 100 mM KCl to the experimental mixture did not affect an appearance and length distribution of the copolymers (data not shown). These results reveal a significant difference in the stability and

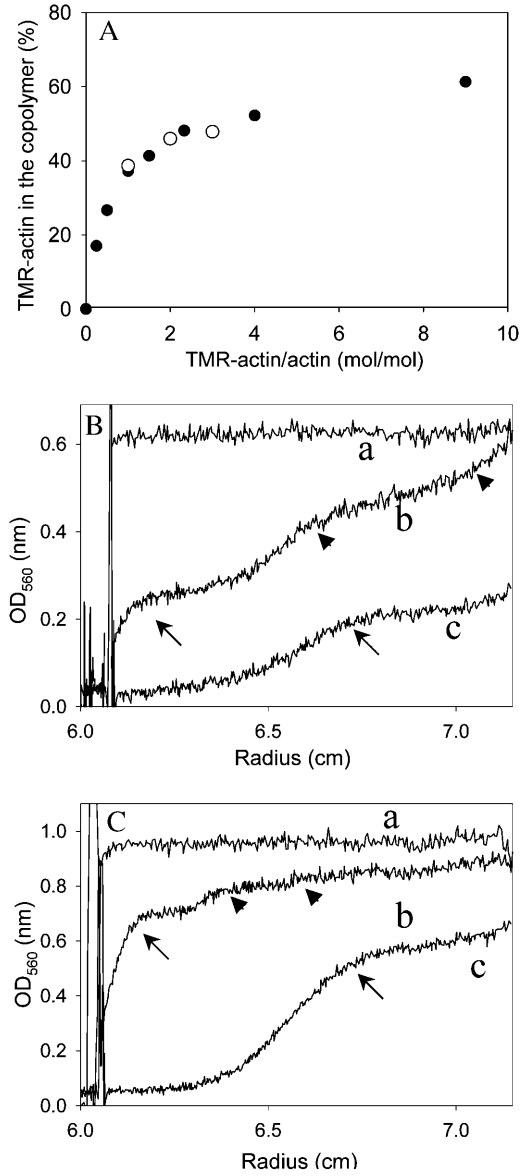

FIGURE 2 (*A*) TMR-actin content in the copolymers with unlabeled actin. TMR-actin content (%) in copolymers was determined as a function of mole ratio of TMR-actin to unmodified actin in the polymerization mixture. The total concentration of actin, polymerized by 2.0 mM $MgCl_2$, was kept constant at 20 μM. TMR-actin incorporation into filaments was determined by sedimentation assays and SDS-PAGE analysis of the fluorescent TMR-actin and total actin in the pellet and supernatant fractions (*solid symbols*) or by analytical ultracentrifugation (*open circles*) (see Materials and Methods). Using Ca- or Mg-G-actin in polymerizations with $MgCl_2$ alone or with 2.0 mM $MgCl_2$ and 100 mM KCl resulted in remarkably similar incorporation of TMR-actin into the copolymers. (*B* and *C*) Analysis of TMR-actin in copolymerization solutions by analytical ultracentrifugation. Sedimentation velocity optical density (*OD*) scans of TMR-actin/unlabeled actin mixtures at 1:1 (*B*) and at 3:1 (*C*) mole ratios in the presence of 2.0 mM $MgCl_2$ were taken at the beginning of the run at 3000 rpm (*a*), after 20-min centrifugation at 30,000 rpm (*b*), and after 159-min centrifugation at 45,000 rpm (*c*). Sedimentation boundaries were recorded at $\lambda = 560$ nm, corresponding to the absorbance maximum of TMR-actin. Shoulders indicated by arrows on scans *b* and *c* correspond to monomer boundaries (3.4S); shoulders indicated by arrowheads in scan *b* correspond to polymer boundaries (~30–90S, with a predominant fraction of ~60S in *B*; and with a predominant fraction of ~35S in *C*). Intermediate-size oligomers were not detected in these sedimentation experiments. The fraction of TMR-actin copolymerized with unlabeled actin was calculated by subtracting the OD of TMR-actin monomers (obtained from the plateau region of curve *c* after correction for radial dilution) from the OD of total sample (*curve a*).

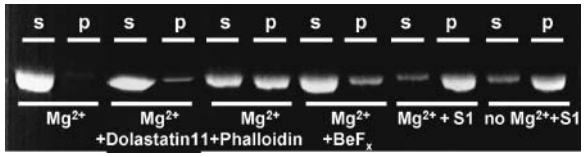

FIGURE 3 Polymerization of TMR-actin in the presence of dolastatin 11, phalloidin, BeFx, and myosin S1. Representative SDS-PAGE patterns of TMR-actin pelleted under different experimental conditions. 10 μM TMR actin was incubated with phalloidin, dolastatin 11, BeF_x, and myosin S1 fragment (10 μM) in the absence or presence of 2.0 mM $MgCl_2$, for 2 h, at 23°C. BeF_x was added to actin as described in Materials and Methods. After ultracentrifugation, the pellet (*p*) and supernatant (*s*) actin fractions were analyzed by SDS-PAGE and visualized under UV light for TMR-actin quantification. Each type of experiment was repeated at least three times with similar results.

flexibility of the control F-actin and the TMR-actin copolymers. In contrast to that, the structure and length distribution of phalloidin-stabilized (Fig. 4 *D*), and S1-decorated (Fig. 4 *C*) TMR-actin filaments did not differ much from the corresponding control filaments.

Light scattering measurements of TMR-actin and unlabeled actin copolymerization

Addition of TMR-actin accelerates the overall rate of polymerization of unlabeled actin by $MgCl_2$ (Fig. 5 *A*). This acceleration is detectable at a mole ratio of 1:11 of TMR-actin to unlabeled actin (0.5 μM and 5.5 μM, respectively), whereas at the 1:5 mol ratio the polymerization is completed ~threefold faster than in unlabeled actin alone (Fig. 5 *A*). Supplementing the polymerization buffer with 100 mM KCl did not affect the polymerization acceleration by TMR-actin (Fig. 5, *A* and *C*), indicating that physiological ionic strength conditions do not significantly stabilize the copolymers. Notably, the acceleration of polymerization induced by TMR-actin was abolished (and even reversed) when either phalloidin or tropomyosin were added to stabilize actin filaments (Fig. 5 *B*). Thus, it appears that the faster polymerization of the copolymers stems from their instability and consequent severing—as documented by electron microscopy (Fig. 4, *B*, *E*, and *F*)—resulting in a higher concentration of free filament ends available for elongation. It has been shown before that cofilin increases the rate of actin polymerization in solution via a similar mechanism (Du and Frieden, 1998; Blanchoin and Pollard, 1999). Although phalloidin also accelerates the polymerization of actin, it does so not by severing filaments (which would be reflected in a characteristic sigmoidal shape of

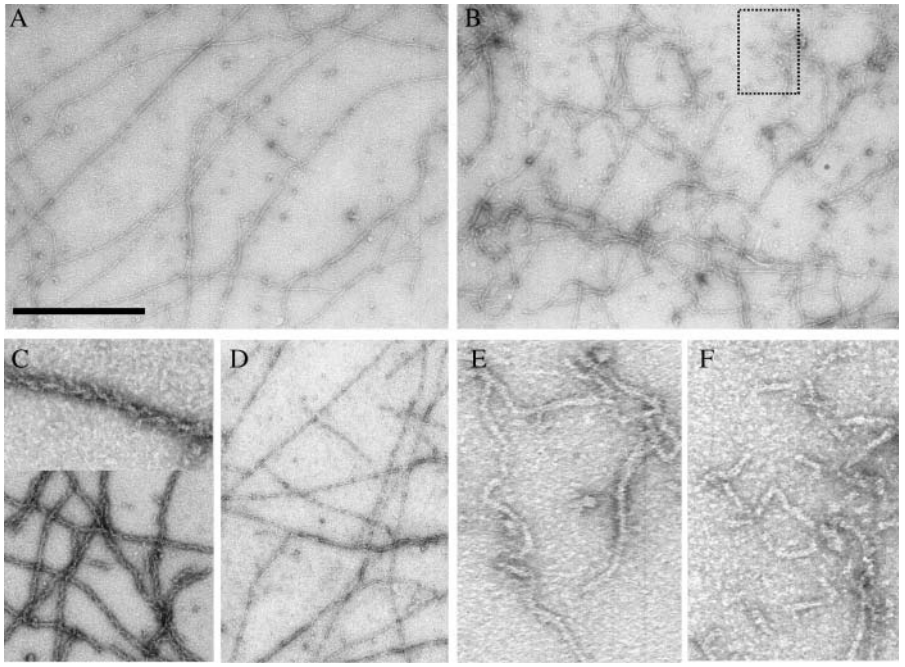

FIGURE 4 Electron microscopy of filaments containing TMR-actin. The polymerization of 5.0 μM unmodified actin (*A*), and a mixture of 5.0 μM TMR-actin and 5.0 μM unmodified actin in the Mg-ATP state (*B*, *E*, and *F*), was initiated by 2.0 mM $MgCl_2$. The copolymerization for 2 h, at room temperature, resulted in filaments containing ~30% of modified actin. Actin samples were applied to EM grids and negatively stained with 1% uranyl acetate (for details see Materials and Methods). *E* and *F* show TMR-actin copolymers at higher magnification. *F* is a fourfold-enlarged image of an area contained in a box in *B*. (*C*) 5.0 μM TMR-actin polymerized by the addition of 5.0 μM myosin S1. Top panel is the higher magnification of a segment in the bottom panel to better show the decoration of TMR-actin filaments with S1 (*D*) 5.0 μM TMR-actin polymerized by the addition of 2.0 mM $MgCl_2$ and 6.0 μM phalloidin. Bar scale corresponds to 500 nm for *A*, *B*, *C* (*bottom panel*), and *D*; 160 nm for *C* (*top panel*); and 125 nm for *E* and *F*.

polymerization curves, as seen on Fig. 5, *A* and *C*), but rather by stabilizing filament nuclei and inhibiting monomer dissociation from filament ends.

In most experiments of this study we used tetramethylrhodamine-5-maleimide (TMR-maleimide) for actin labeling. However, tetramethylrhodamine-5-iodoacetamide (TMR-iodoacetamide)-modified actin was used in many prior investigations to visualize actin filaments (Tait and Frieden, 1982; Sund and Axelrod, 2000; Adami et al., 2002; Cintio et al., 2001). To confirm that our results are relevant also to other rhodamine derivatives attached to the Cys^{374} of actin, we prepared TMR-iodoacetamide-actin and compared it to TMR-maleimide-actin in light scattering experiments. Both TMR-maleimide- and TMR-iodoacetamide-modified actins (20% of total actin) accelerate actin polymerization in a similar way (Fig. 5 *C*), suggestive of filament severing and similar properties of these actins.

Thermostability of the TMR-actin/unlabeled actin copolymers

Differential scanning calorimetry (DSC) did not reveal any significant difference between the thermal transition temperatures of TMR-modified and unlabeled Ca^{2+}-G-actins (64.6 $\pm$ 0.9 and 64.0 $\pm$ 0.7°C, respectively). The thermal transition of Mg-TMR-actin was at a lower temperature (56.6 $\pm$ 0.7°C) than that of Ca-TMR actin. The melting of unlabeled Mg-G-actin could not be measured reliably because of its tendency to oligomerize at concentrations much lower (12.5 μM; Attri et al., 1991) than those used in the DSC (60 μM).

Filaments of unlabeled actin have a similar melting temperature irrespective of the divalent cation (Ca^{2+} or Mg^{2+}) bound at the high affinity site of actin monomers (70.2 $\pm$ 0.3 and 70.3 $\pm$ 0.7°C, respectively), although Mg^{2+}-actin shows somewhat lower enthalpy and cooperativity of heat capacity profiles. Both Ca^{2+} and Mg^{2+} copolymers of unlabeled actin and TMR-actin are destabilized, albeit unequally, with the increasing content of TMR-actin (Fig. 6 *A*). The destabilization of Mg^{2+}-copolymers is significantly stronger than that of Ca^{2+}-copolymers (Fig. 6, *A–B*). This difference cannot be attributed to a different content of TMR-actin in the filaments (28.3 $\pm$ 2.2 and 30.7 $\pm$ 1.6% of TMR-actin in the Ca^{2+} and Mg^{2+} copolymers, respectively). Moreover, electron microscopy observation of these filaments did not reveal any significant morphological differences between them. Although heat consumption profiles for copolymer melting could not be fitted to a single Gaussian peak, they were very similar to the profiles recorded for homopolymers of unlabeled actin (Fig. 6 *C*), indicating their homogenous behavior in terms of thermal stability. The addition of KCl increased slightly the thermal stability of the copolymers and the cooperativity of the transition irrespective of the high affinity divalent cation bound to actin (Fig. 6 *B*).

DISCUSSION

In contrast to phalloidin-based labels, which bind only to F-actin and stabilize it, rhodamine derivatives attached to Cys-374 on actin proved to be helpful in investigating the dynamic behavior of actin filaments (Amann and Pollard, 2001; Fujiwara et al., 2002a,b). However, we show here that

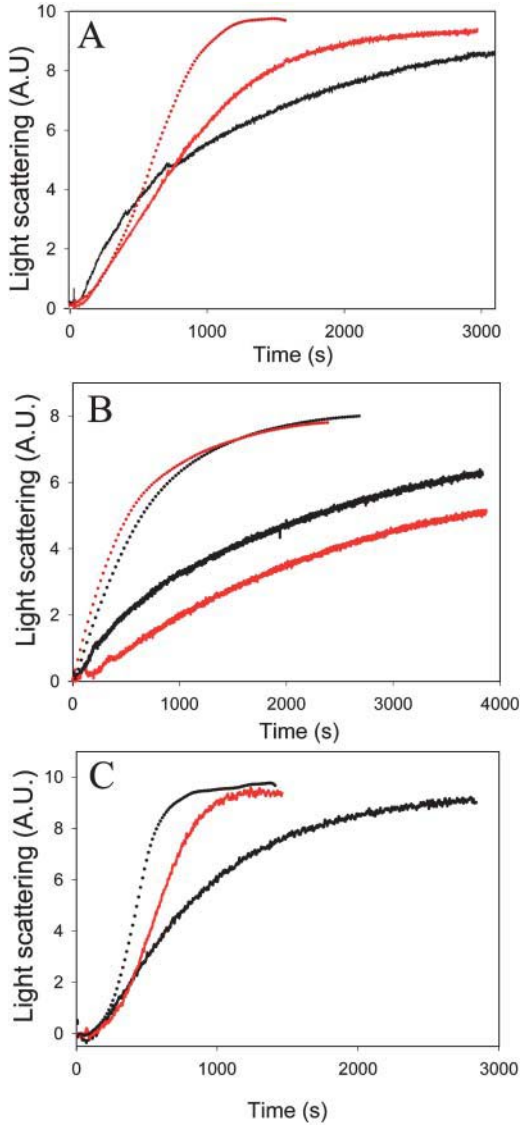

FIGURE 5 Copolymerization of mixtures of unlabeled and TMR-labeled actin. The polymerization of unlabeled actin, and mixtures of unlabeled actin with TMR-actin in the presence and absence of actin-binding proteins and phalloidin was monitored via the increase in light scattering at $\lambda = 350$ nm. (*A*) The polymerization of 6.0 μM unlabeled actin (*solid black line*), 5.5 μM unlabeled actin and 0.5 μM TMR-actin mixture (*solid red line*), and 5.0 μM unlabeled actin and 1.0 μM TMR-actin mixture (*dotted red line*), all in Mg-ATP state, was initiated by the addition of 2.0 mM $MgCl_2$. Note that the initial stage of polymerization is slower in the presence of TMR-actin. (*B*) The polymerization of 6.0 μM unlabeled actin (*black lines*), and 5.0 μM unlabeled actin/1.0 μM TMR-actin mixture (*red lines*), in the presence of either 1.5 μM tropomyosin (*solid lines*) or 6.0 μM phalloidin (*dotted lines*), was initiated by 2.0 mM $MgCl_2$. (*C*) The polymerization of 5 μM unlabeled actin (*solid black line*), mixture of 4 μM unlabeled actin/1 μM TMR-maleimide-labeled actin (*solid red line*), and actin labeled with TMR-iodacetamide with 20% efficiency (*dotted black line*), all in Mg-ATP state, was initiated by simultaneous addition of 2 mM $MgCl_2$ and 100 μM KCl.

the copolymerization of TMR-actin with unlabeled actin alters filament structure and dynamics in proportion to the fraction of TMR-actin in the copolymers.

TMR-actin mimics the severing effect of cofilin on F-actin

As shown in Fig. 1, TMR-actin neither nucleates new filaments nor elongates the preformed nuclei into filaments unless it is stabilized by phalloidin, myosin S1, or the presence of unlabeled actin. In the latter case, unlabeled actin and TMR-actin copolymerize with a maximum incorporation of ~50% of labeled actin out of the total actin in the copolymer. This indicates that on average the unlabeled actin molecules may alternate with TMR-actin protomers, thereby decreasing the structural strain due to perturbations in the interprotomer contacts (that preclude filament existence with TMR-actin alone). The resulting TMR-copolymers are intrinsically unstable and show increased fragmentation, probably due to the accumulated structural strain (Figs. 4 and 5). In this sense, TMR-actin mimics the action of severing proteins. For cofilin, the main member of this class of proteins, filaments fragmentation has indeed been linked to the changes in lateral and longitudinal interprotomer contacts in F-actin (McGough et al., 1997; McGough and Chiu, 1999; Galkin et al., 2002, 2003; Bobkov et al., 2002, 2004). Also, similarly to cofilin, TMR-actin accelerates the polymerization of actin in solution (Fig. 5) by increasing the number of filament ends available for elongation.

TMR-actin accelerates the polymerization of unlabeled actin in solution

Our electron microscopy images reveal that TMR-actin shortens and impairs the structure of copolymers compared to control filaments. In principle, short copolymers (Fig. 4) could be produced if TMR-actin had increased the nucleation of actin filaments (Tait and Frieden, 1982). However, two sets of data show that this is not the case: 1), analytical ultracentrifugation did not detect any oligomeric species in solutions of TMR-actin alone (in the presence of 2 mM $MgCl_2$) nor in copolymer solutions; and 2), addition of TMR-actin to unlabeled actin does not accelerate, but instead delays the beginning of polymerization, indicating the inhibition of filament nucleation. After that initial period, TMR-actin speeds up the polymerization, as reflected in the sigmoidal polymerization curves (Fig. 5 *A*). Notably, the acceleration of polymerization at low ratios of TMR-actin/unlabeled actin is most evident when using gel-filtered actin. In the unfiltered actin, traces of oligomers and actin-binding proteins accelerate the nucleation (resulting in shorter filaments) and mask the effect of TMR-actin.

The kinetics of a similar, cofilin-dependent acceleration of actin polymerization (Du and Frieden, 1998; Blanchoin and Pollard, 1999) was fitted well to a scheme assuming filament

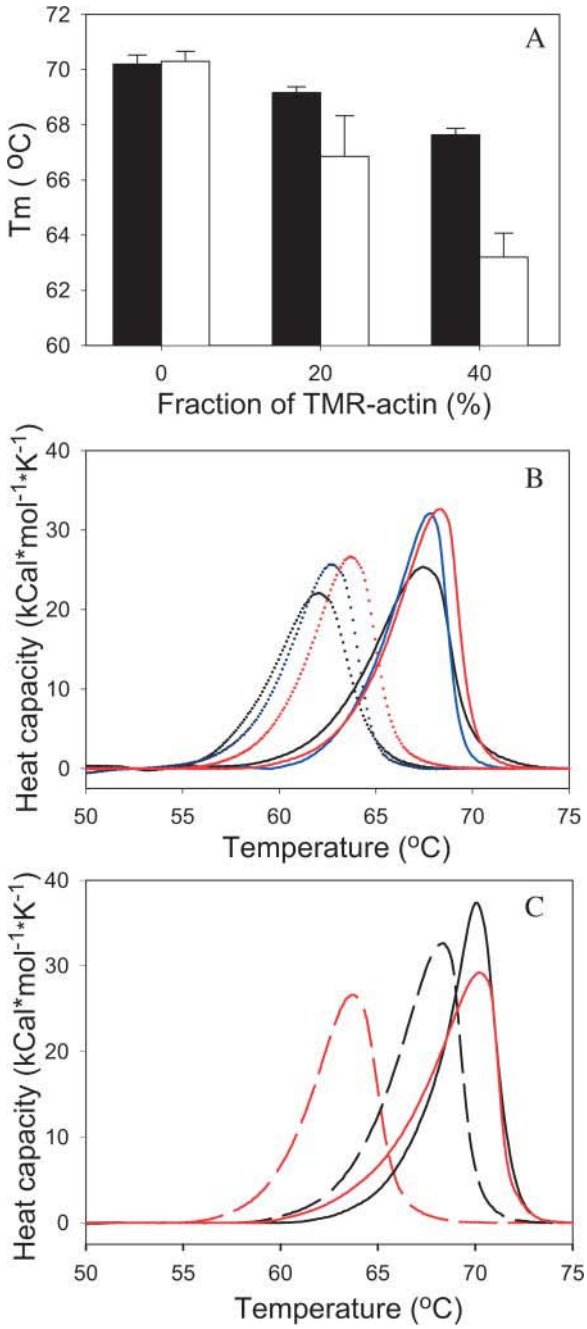

FIGURE 6 Differential scanning calorimetry of TMR-actin copolymers. (*A*) Thermal transition temperatures versus TMR-actin content (%). 60 μM Ca^{2+}-G-actin (*solid columns*) or Mg^{2+}-actin (*open columns*) were polymerized by 100 mM KCl for 2 h, at room temperature, and then analyzed by DSC. Bars represent standard deviations of three independent experiments. (*B*) Representative heat capacity peaks for 60 μM TMR-actin copolymers at (3:2 mole ratio of unlabeled actin/TMR-actin) with Ca^{2+} (*solid lines*) and Mg^{2+} (*dotted lines*) bound at the high affinity binding site. Actin samples were polymerized with 2.0 mM Ca^{2+}- or Mg^{2+}- (*black lines*), 100 mM KCl (*blue lines*), or with both 2.0 mM divalent cation and 100 mM KCl (*red lines*). (*C*) Representative heat absorption peaks of Ca^{2+} (*black lines*) or Mg^{2+} (*red lines*) F-actin polymerized by 100 mM KCl and the corresponding divalent cation (2.0 mM). Solid lines represent unlabeled actin; dashed lines are for a 3:2 mol ratio of unlabeled actin/TMR-actin.

fragmentation by cofilin (Du and Frieden, 1998). The addition of tropomyosin and/or phalloidin, both of which are well known to stabilize F-actin, abolished the TMR-actin-induced acceleration of polymerization. This is consistent with filament severing being the mechanism by which TMR-actin speeds up actin polymerization. Therefore, our data strongly suggest that TMR-actin severs the copolymers, producing additional filament ends, which participate in filament elongation. These data agree well with the recent studies of Adami et al. (2002, 2003), who show that the yield strength of tropomyosin-stabilized filaments of unlabeled actin is ~fivefold higher than that of tropomyosin-stabilized TMR-actin copolymers, which, in turn, is ~threefold higher than the yield strength of TMR-actin/unlabeled actin copolymers in the absence of tropomyosin (50.5 pN, 10 pN, and 3.5 pN, respectively).

Recently, taking advantage of total internal reflection fluorescence microscopy, TMR-actin was used at a 1:9 mol ratio to unlabeled actin to image the in vitro actin filaments growth and treadmilling (Fujiwara et al., 2002b). The analysis of length fluctuation of individual filaments led to the unexpected conclusions that the elongation and dissociation constants (k^+ and k^-) are ~40 times higher at steady state than during the elongation step (Fujiwara et al., 2002b). To explain this difference, the assumption was made that hexamers—and not monomers—are the average effective size units of elongation/dissociation at the steady state treadmilling (Fujiwara et al., 2002b). Our results point to the possibility that the suggested putative hexamers dissociation is an artifact of TMR-actin presence in the copolymers and not an intrinsic property of actin itself. Although Fujiwara et al. (2002b) did not observe filament fragmentation at TMR-actin/unlabeled actin ratio similar to that used in this study (1:11; Fig. 5 *A*), the copolymers in the former case might have been stabilized through contacts with the glass surface of the coverslip. It is also possible that fragmentation could have escaped detection in that study if it occurred mainly at the pointed ends of filaments, where the contacts between subdomains 1 and 2 of two longitudinally adjacent actin protomers are strongly weakened or even disrupted (Galkin et al., 2003). The extent of such a conformational perturbation was estimated to span ~10 monomers from the pointed end (Galkin et al., 2003), which correlates with the hexamer treadmilling unit suggested by Fujiwara et al. (2002b).

Factors stabilizing TMR-actin filaments

In addition to the copolymerization with unlabeled actin, TMR-actin can be stabilized in the F-actin form by myosin S1 and phalloidin, but not by dolastatin 11 (Fig. 3). Recently, dolastatin 11 was shown to strongly stabilize F-actin, similarly to phalloidin, by intercalating between the two long pitch strands of filaments (Oda et al., 2003; Bai et al., 2001). However, in contrast to phalloidin, which was mapped to the interface among three adjacent protomers

($n-1$, n, and $n+1$; Steinmetz et al., 1998), dolastatin 11 makes contacts with only two laterally adjacent protomers (n and $n+1$). The difference in dolastatin 11 and phalloidin contacts with actin appears critical to the TMR-actin polymerization. This can be explained by assuming that phalloidin stabilizes both lateral and longitudinal (inter- and intrastrand) contacts, whereas dolastatin 11 is able to stabilize mainly lateral contacts—which is not enough to allow TMR-actin assembly into filaments. Moreover, because it does not bind to actin monomers, phalloidin must stabilize otherwise unstable and transient oligomers of the TMR-actin to assist in their polymerization.

The efficient polymerization of TMR-actin in the presence of myosin S1 may reflect the restoration of normal longitudinal inter-actin contacts by S1 (Fig. 3). It has been shown that S1-induced assembly of G-actin into filaments begins with longitudinal bridging of two actin molecules by one S1 molecule, followed by their further condensation into higher oligomers and polymers (Valentin-Ranc et al., 1991; Valentin-Ranc and Carlier, 1992; Fievez et al., 1997; Blanchoin et al., 1995). Similar rates of S1-induced polymerization of unlabeled and TMR-actin (data not shown) suggest that the same mechanism of filaments assembly is involved in both cases. However, the TMR-actin filaments depend on S1 for their stability and existence, and disassemble almost immediately upon addition of ATP (and the consequent dissociation of S1), whereas the destabilization of unlabeled actin filaments is much slower. This suggests that S1 may be stabilizing weakly connected protomers in TMR-F-actin by bridging over incompatible interfaces.

Alternatively, and more generally, the polymerization of TMR-actin by phalloidin and/or S1 may be facilitated by allosteric changes in the position of the TMR-label, decreasing its inhibitory effect on actin polymerization and forcing TMR-actin into normal F-actin conformation. The destabilization and severing of actin filaments by TMR-actin, as well as the antagonistic effects of filament stabilizing factors to such action are reminiscent of the effects of cofilin on actin filaments. It will be interesting to test the possibility that the disruption of filaments by ADF/cofilin proteins and TMR-actin have a similar structural basis, perhaps related to an intrinsic mode of F-actin instability (Galkin et al., 2003).

We thank Dr. Albina Orlova (University of Virginia, Charlottesville, VA) for help with the preparation of electron micrographs and Dr. Robert Bates (University of Arizona, Tucson, AZ) for a generous gift of dolastatin 11. We thank Drs. Edward Egelman (University of Virginia) and Albina Orlova for valuable discussions.

This work was supported by grants from the United States Public Health Service (AR 22031) and the National Science Foundation (MCB 0316269).

REFERENCES

Adami, R., O. Cintio, G. Trombetta, D. Choquet, and E. Grazi. 2002. Effects of chemical modification, tropomyosin, and myosin subfragment 1 on the yield strength and critical concentration of F-actin. *Biochemistry.* 41:5907–5912.

Adami, R., O. Cintio, G. Trombetta, D. Choquet, and E. Grazi. 2003. On the stiffness of the natural actin filament decorated with alexa fluor tropomyosin. *Biophys. Chem.* 104:469–476.

Aizawa, H., M. Sameshima, and I. Yahara. 1997. A green fluorescent protein actin fusion protein dominantly inhibits cytokinesis, cell spreading, and locomotion in *Dictyostelium*. *Cell Struct. Funct.* 22: 335–345.

Amann, K. J., and T. D. Pollard. 2001. Direct real-time observation of actin filament branching mediated by Arp2/3 complex using total internal reflection fluorescence microscopy. *Proc. Natl. Acad. Sci. USA.* 98: 15009–15013.

Attri, A. K., M. S. Lewis, and E. D. Korn. 1991. The formation of actin oligomers studied by analytical ultracentrifugation. *J. Biol. Chem.* 266: 6815–6824.

Bai, R. L., P. Verdier-Pinard, S. Gangwar, C. C. Stessman, K. J. McClure, E. A. Sausville, G. R. Pettit, R. B. Bates, and E. Hamel. 2001. Dolastatin 11, a marine depsipeptide, arrests cells at cytokinesis and induces hyperpolymerization of purified actin. *Mol. Pharmacol.* 59:462–469.

Bernstein, B. W., and J. R. Bamburg. 1992. Actin in emerging neurites is recruited from A monomer pool. *Mol. Neurobiol.* 6:95–106.

Blanchoin, L., S. Fievez, F. Travers, M. F. Carlier, and D. Pantaloni. 1995. Kinetics of the interaction of myosin subfragment-l with G-actin. *J. Biol. Chem.* 270:7125–7133.

Blanchoin, L., and T. D. Pollard. 1999. Mechanism of interaction of *Acanthamoeba actophorin* (ADF/cofilin) with actin filaments. *J. Biol. Chem.* 274:15538–15546.

Bobkov, A. A., A. Muhlrad, K. Kokabi, S. Vorobiev, S. C. Almo, and E. Reisler. 2002. Structural effects of cofilin on longitudinal contacts in F-actin. *J. Mol. Biol.* 323:739–750.

Bobkov, A. A., A. Muhlrad, A. Shvetsov, S. Benchaar, D. Scoville, S. C. Almo, and E. Reisler. 2004. Cofilin (ADF) affects lateral contacts in F-actin. *J. Mol. Biol.* 337:93–104.

Choidas, A., A. Jungbluth, A. Sechi, J. Murphy, A. Ullrich, and G. Marriott. 1998. The suitability and application of a GFP-actin fusion protein for long-term imaging of the organization and dynamics of the cytoskeleton in mammalian cells. *Eur. J. Cell Biol.* 77:81–90.

Cintio, O., R. Adami, D. Choquet, and E. Grazi. 2001. On the elastic properties of tetramethylrhodamine F-actin. *Biophys. Chem.* 92:201–207.

Du, J. Y., and C. Frieden. 1998. Kinetic studies on the effect of yeast cofilin on yeast actin polymerization. *Biochemistry.* 37:13276–13284.

Estes, J. E., L. A. Selden, H. J. Kinosian, and L. C. Gershman. 1992. Tightly-bound divalent cation of actin. *J. Mus. Res. Cell Motil.* 13: 272–284.

Fievez, S., D. Pantaloni, and M. F. Carlier. 1997. Kinetics of myosin subfragment-1-induced condensation of G-actin into oligomers, precursors in the assembly of F-actin-S-1. Role of the tightly bound metal ion and ATP hydrolysis. *Biochemistry.* 36:11837–11842.

Frieden, C. 1983. Polymerization of actin mechanism of the Mg^{2+}-induced process at pH −8 and 20°C. *Proc. Natl. Acad. Sci. USA.* 80:6513–6517.

Fujiwara, I., S. Suetsugu, S. Uemura, T. Takenawa, and S. Ishiwata. 2002a. Visualization and force measurement of branching by Arp2/3 complex and N-WASP in actin filament. *Biochem. Biophys. Res. Commun.* 293:1550–1555.

Fujiwara, I., S. Takahashi, H. Tadakuma, T. Funatsu, and S. Ishiwata. 2002b. Microscopic analysis of polymerization dynamics with individual actin filaments. *Nat. Cell Biol.* 4:666–673.

Fukui, Y., E. de Hostos, S. Yumura, T. Kitanishi-Yumura, and S. Inoue. 1999. Architectural dynamics of F-actin in *eupodia* suggests their role in invasive locomotion in *Dictyostelium*. *Exp. Cell Res.* 249:33–45.

Galkin, V. E., M. S. Vanloock, A. Orlova, and E. H. Egelman. 2002. A new internal mode in F-actin helps explain the remarkable evolutionary conservation of actin's sequence and structure. *Curr. Biol.* 12:570–575.

Galkin, V. E., A. Orlova, M. S. Vanloock, A. Shvetsov, E. Reisler, and E. H. Egelman. 2003. ADF/cofilin use an intrinsic mode of F-actin instability to disrupt actin filaments. *J. Cell Biol.* 163:1057–1066.

Gilbert, H. R., and C. Frieden. 1983. Preparation, purification and properties of a crosslinked trimer of G-actin. *Biochem. Biophys. Res. Commun.* 111:404–408.

Godfrey, J. E., and W. F. Harrington. 1970. Self-association in the myosin system at high ionic strength. *Biochemistry.* 9:894–908.

Hamaguchi, Y., and I. Mabuchi. 1988. Accumulation of fluorescently labeled actin in the cortical layer in sea-urchin eggs after fertilization. *Cell Motil. Cytoskeleton.* 9:153–163.

Hegyi, G., M. Mak, E. Kim, M. Elzinga, A. Muhlrad, and E. Reisler. 1998. Intrastrand cross-linked actin between Gln^{41} and Cys^{374}. I. Mapping of sites cross-linked in F-actin by *n*-(4-azido-2-nitrophenyl) putrescine. *Biochemistry.* 37:17784–17792.

Hosein, R. E., S. A. Williams, K. Haye, and R. H. Gavin. 2003. Expression of GFP-actin leads to failure of nuclear elongation and cytokinesis in *Tetrahymena thermophila*. *J. Eukaryot. Microbiol.* 50:403–408.

Kreis, T. E., B. Geiger, and J. Schlessinger. 1982. Mobility of microinjected rhodamine actin within living chicken gizzard cells determined by fluorescence photobleaching recovery. *Cell.* 29:835–845.

Kudryashov, D. S., and E. Reisler. 2003. Solution properties of tetramethylrhodamine-modified G-actin. *Biophys. J.* 85:2466–2475.

Laemmli, U. K. 1970. Cleavage of structural proteins during the assembly of the head of bacteriophage T4. *Nature.* 227:680–685.

MacLean-Fletcher, S., and T. D. Pollard. 1980. Identification of a factor in conventional muscle actin preparations which inhibits actin filament self-association. *Biochem. Biophys. Res. Commun.* 96:18–27.

McGough, A., B. Pope, W. Chiu, and A. Weeds. 1997. Cofilin changes the twist of F-actin: implications for actin filament dynamics and cellular function. *J. Cell Biol.* 138:771–781.

McGough, A., and W. Chiu. 1999. ADF/cofilin weakens lateral contacts in the actin filament. *J. Mol. Biol.* 291:513–519.

Miller, L., M. Phillips, and E. Reisler. 1988. Polymerization of G-actin by myosin subfragment-1. *J. Biol. Chem.* 263:1996–2002.

Nishida, E., K. Iida, N. Yonezawa, S. Koyasu, I. Yahara, and H. Sakai. 1987. Cofilin is a component of intranuclear and cytoplasmic actin rods induced in cultured cells. *Proc. Natl. Acad. Sci. USA.* 84:5262–5266.

Nwe, T. M., and Y. Shimada. 2000. Inhibition of nebulin and connectin (titin) for assembly of actin filaments during myofibrillogenesis. *Tissue Cell.* 32:223–227.

Oda, T., Z. D. Crane, C. W. Dicus, B. A. Sufi, and R. B. Bates. 2003. Dolastatin 11 connects two long-pitch strands in F-actin to stabilize microfilaments. *J. Mol. Biol.* 328:319–324.

Otterbein, L. R., P. Graceffa, and R. Dominguez. 2001. The crystal structure of uncomplexed actin in the ADP state. *Science.* 293:708–711.

Sept, D., and J. A. McCammon. 2001. Thermodynamics and kinetics of actin filament nucleation. *Biophys. J.* 81:667–674.

Spudich, J. A., and S. Watt. 1971. The regulation of rabbit skeletal muscle contraction. I. Biochemical studies of the interaction of the tropomyosin-troponin complex with actin and the proteolytic fragments of myosin. *J. Biol. Chem.* 246:4866–4871.

Steinmetz, M. O., D. Stoffler, S. A. Muller, W. Jahn, B. Wolpensinger, K. N. Goldie, A. Engel, H. Faulstich, and U. Aebi. 1998. Evaluating atomic models of F-actin with an undecagold-tagged phalloidin derivative. *J. Mol. Biol.* 276:1–6.

Sund, S. E., and D. Axelrod. 2000. Actin dynamics at the living cell submembrane imaged by total internal reflection fluorescence photobleaching. *Biophys. J.* 79:1655–1669.

Tait, J. F., and C. Frieden. 1982. Chemical modification of actin—acceleration of polymerization and reduction of network formation by reaction with *n*-ethylmaleimide, (iodoacetamido)tetramethylrhodamine, or 7-chloro-4-nitro-2,1,3-benzoxadiazole. *Biochemistry.* 21:6046–6053.

Tobacman, L. S., and E. D. Korn. 1983. The kinetics of actin nucleation and polymerization. *J. Biol. Chem.* 258:3207–3214.

Tsuda, Y., H. Yasutake, A. Ishijima, and T. Yanagida. 1996. Torsional rigidity of single actin filaments and actin-actin bond breaking force under torsion measured directly by in vitro micromanipulation. *Proc. Natl. Acad. Sci. USA.* 93:12937–12942.

Valentin-Ranc, C., C. Combeau, M. F. Carlier, and D. Pantaloni. 1991. Myosin subfragment-1 interacts with 2 G-actin molecules in the absence of ATP. *J. Biol. Chem.* 266:17872–17879.

Valentin-Ranc, C., and M. F. Carlier. 1992. Characterization of oligomers as kinetic intermediates in myosin subfragment 1-induced polymerization of G-actin. *J. Biol. Chem.* 267:21543–21550.

Weeds, A. G., and B. Pope. 1977. Studies on chymotryptic digestion of myosin—effects of divalent cations on proteolytic susceptibility. *J. Mol. Biol.* 111:129–157.

Westphal, M., A. Jungbluth, M. Heidecker, B. Muhlbauer, C. Heizer, J. M. Schwartz, G. Marriott, and G. Gerisch. 1997. Microfilament dynamics during cell movement and chemotaxis monitored using a GFP-actin fusion protein. *Curr. Biol.* 7:176–183.

Yonezawa, N., E. Nishida, S. Maekawa, and H. Sakai. 1988. Studies on the interaction between actin and cofilin purified by a new method. *Biochem. J.* 251:121–127.

Yumura, S., and Y. Fukui. 1998. Spatiotemporal dynamics of actin concentration during cytokinesis and locomotion in *Dictyostelium*. *J. Cell Sci.* 111:2097–2108.